JOURNAL OF MORPHOLOGY 276:550–563 (2015)

Functional Skeletal Morphology and Its Implications for Locomotory Behavior Among Three Genera of Myosoricine Shrews (Mammalia: Eulipotyphla: Soricidae)

Neal Woodman[1]* and Frank A. Stabile[2]

[1]*Department of Vertebrate Zoology, USGS Patuxent Wildlife Research Center, National Museum of Natural History, Smithsonian Institution, Washington, DC 20013-7012*
[2]*Department of Biology, The College of New Jersey, Ewing, New Jersey 08628*

ABSTRACT Myosoricinae is a small clade of shrews (Mammalia, Eulipotyphla, Soricidae) that is currently restricted to the African continent. Individual species have limited distributions that are often associated with higher elevations. Although the majority of species in the subfamily are considered ambulatory in their locomotory behavior, species of the myosoricine genus *Surdisorex* are known to be semifossorial. To better characterize variation in locomotory behaviors among myosoricines, we calculated 32 morphological indices from skeletal measurements from nine species representing all three genera that comprise the subfamily (i.e., *Congosorex*, *Myosorex*, *Surdisorex*) and compared them to indices calculated for two species with well-documented locomotory behaviors: the ambulatory talpid *Uropsilus soricipes* and the semifossorial talpid *Neurotrichus gibbsii*. We summarized the 22 most complete morphological variables by 1) calculating a mean percentile rank for each species and 2) using the first principal component from principal component analysis of the indices. The two methods yielded similar results and indicate grades of adaptations reflecting a range of potential locomotory behaviors from ambulatory to semifossorial that exceeds the range represented by the two talpids. Morphological variation reflecting grades of increased semifossoriality among myosoricine shrews is similar in many respects to that seen for soricines, but some features are unique to the Myosoricinae. J. Morphol. 276:550–563, 2015.

KEY WORDS: anatomy; digging; fossorial; Insectivora; Soricomorpha; substrate use; terrestrial

INTRODUCTION

Shrews (Mammalia: Eulipotyphla: Soricidae) exhibit a limited range of locomotory behaviors and substrate use. Most soricids are classified as terrestrial, ambulatory predators that forage predominantly on epigeal invertebrates. Only about 10% of shrews are considered semifossorial, and a few other species are scansorial or semiaquatic (Hutterer, 1985; Churchfield, 1990). Despite the predominance of ambulatory behavior in the family, semifossorial species occur in all three soricid subfamilies and are geographically widespread (Hutterer, 1985; Churchfield, 1990). Paradoxically, even ambulatory soricids possess a number of external characters that are common to semifossorial and fossorial mammals. These include a fusiform body with short, dense fur; short, stout limbs; and small pinnae and eyes (Shimer, 1903; Eisenberg, 1981; Churchfield, 1990; Stein, 2000). Variation in soricid skeletal characteristics that are typically tied to locomotory behavior suggests that substrate use is more nuanced and diverse than is recognized by standard stereotypical categories (Woodman and Gaffney, 2014).

Myosoricinae is a clade (Quérouil et al., 2001; Willows-Munro and Matthee, 2011) of small- to medium-bodied African shrews that comprises at least 19 species of Mouse Shrews and Forest Shrews (genus *Myosorex* Gray, 1838), three species of Mole Shrews (*Surdisorex* Thomas, 1906), and three species of Congo Shrews (*Congosorex* Heim de Balsac and Lamotte, 1956; Meester, 1953;

Additional Supporting Information may be found in the online version of this article.

Contract grant sponsor: National Science Foundation [through the Natural History Research Experiences Program of the United States National Museum of Natural History (USNM) (to F.A.S)].

*Correspondence to: Neal Woodman, USGS Patuxent Wildlife Research Center, National Museum of Natural History, MRC 111, Smithsonian Institution, PO Box 37012, Washington, DC 20013-7012. E-mail: woodmann@si.edu

Frank A. Stabile is currently at Department of Ecology & Evolutionary Biology, Yale University, New Haven, CT 06511.

Received 4 August 2014; Revised 9 December 2014;
Accepted 19 December 2014.

Published online 10 February 2015 in
Wiley Online Library (wileyonlinelibrary.com).
DOI 10.1002/jmor.20365

Fig. 1. Anterior aspect of left humeri of nine myosoricine shrews and two moles. Shrews: (**A**) *M. cafer* (FM 165585); (**B**) *M. kihaulei* (FM 204860); (**C**) *M. geata* (FM 197673); (**D**) *C. phillipsorum* (FM 177689); (**E**) *M. varius* (FM 165592); (**F**) *M. blarina* (FM 144209); (**G**) *M. zinki* (FM 174117); (**H**) *S. polulus* (USNM 589820); (**I**) *S. norae* (USNM 589817). Moles: (**J**) *U. soricipes* (USNM 574297); and (**K**) *N. gibbsii* (USNM 273085).

Hutterer, 2005; Stanley et al., 2005; Kerbis Peterhans et al., 2008, 2009, 2010, 2013; Taylor et al., 2013). Most myosoricines have limited geographical distributions in regions that are difficult to access, and their ecology, substrate use, and locomotory behavior remain poorly documented. Species of *Myosorex* are generally considered to be ambulatory, whereas species of *Surdisorex* are known to be semifossorial (Duncan and Wrangham, 1971; Coe and Foster, 1972; Hutterer, 1985). Our early observations indicated that locomotory differences between these two genera are reflected to some extent in external morphological characteristics, including the relative dimensions of the palm, digits, and claws of the forefeet (Woodman and Stabile, 2015). Subsequent inspection of postcranial skeletons of *Myosorex* and *Surdisorex* revealed abundant variation (Fig. 1). External and skeletal differences just within the genus *Myosorex* suggested the potential for a broader diversity of locomotory behaviors than is currently recognized.

In the absence of direct behavioral observations for most myosoricines, we investigated the potential for using skeletal morphology to assess locomotory mode. We studied and measured skeletal elements from nine myosoricine species representing all three genera and calculated 32 morphological indices from them. Most of these indices derive from previous studies of a variety of other mammals and were designed to aid in understanding locomotory adaptations (Price, 1993; Lemelin, 1999; Sargis, 2002; Weisbecker and Warton, 2006; Weisbecker and Schmid, 2007; Kirk et al., 2008; Samuels and Van Valkenburgh, 2008; Hopkins and Davis, 2009; Elissamburu and De Santis, 2011; Woodman and Gaffney, 2014). We statistically summarized these indices and constructed a relative scale to provide a predictive measure of locomotory behavior from ambulatory to semifossorial. Herein, we evaluate the relative locomotory behavior of each species based on this scale and summarize skeletal changes that accompany increased semifossoriality in the myosoricine clade.

MATERIALS AND METHODS

Because of their small size, individual bones of soricids are difficult to manipulate and measure accurately or precisely with hand-held calipers. Instead, the scapula, humerus, ulna, radius, femur, and tibiofibula were digitally photographed. The resulting images were imported into Adobe Photoshop CS3 Extended 10.0.1 (Adobe Systems, San Jose, CA), and 21 variables (Fig. 2) were measured using the Custom Measuring Scale in the Analysis menu following Woodman and Gaffney (2014).

Following the procedures outlined in Woodman and Morgan (2005; see also Woodman and Stephens, 2010; Sargis et al., 2013a, 2013b), we obtained digital x-ray images of the bones of the manus and the pes by x-raying feet of dried skins using a Kevex X-Ray Source 4.1.3 (Kevex, Palo Alto, CA) with Varian Image Viewing and Acquisition 2.0 software (VIVA, Waltham, MA) in the Division of Fishes, National Museum of Natural History, Washington, DC. We imported the resulting images into Adobe Photoshop CS3 Extended and measured lengths and widths from each of the bones and claws of the five rays of the manus and from ray III of the pes (Fig. 3). "Digit" herein refers to the bones and tissues associated with the phalanges, and "ray" refers to those associated with the phalanges and metacarpal. As a proxy for body size, we calculated head-and-body length (HB) by subtracting tail length from total length as recorded by the original collectors. All measurements are reported in mm and are summarized in Supporting Information Supplement 1.

We measured 87 individuals representing three genera and nine species of myosoricine shrews. Specimens used in this study (Appendix) are deposited in the following institutions: American Museum of Natural History, New York, NY; Field Museum of Natural History, Chicago, IL; National Museum of Natural History, Washington, DC. Sample sizes were limited by the availability of skeletons (Bell and Mead, 2014). To better understand the differences in skeletal characters distinguishing terrestrial and semifossorial species of shrews, we measured 10 specimens of the ambulatory Chinese Shrew-mole, *Uropsilus soricipes* Milne-Edwards, 1871 and 26 specimens of the semifossorial Shrew-mole, *Neurotrichus gibbsii* (Baird, 1857). Moles (Talpidae) are a likely sister-group to shrews (Meredith et al., 2011), and their adaptations for semifossorial and fossorial locomotion and substrate use are well documented (e.g., Edwards, 1937; Sanchez-Villagra et al., 2004).

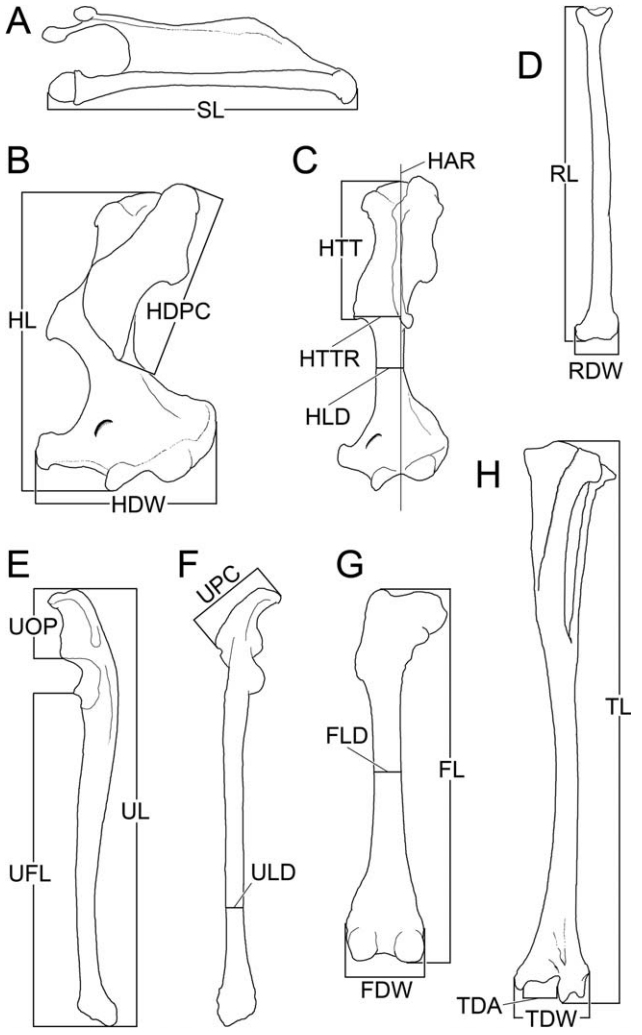

Fig. 2. Measurements of the long bones of the postcranial skeleton. (**A**) Posterior aspect of left scapula: SL, greatest length of scapula. (**B**) Anterior aspect of left humerus: HL, length of humerus; HDW, distal width of humerus (epicondylar breadth); HDPC, length of deltopectoral crest. (**C**) Anterior aspect of left humerus: HAR, axis of rotation of the humerus; HLD, least mediolateral diameter of humerus; HTT, length from head of humerus to distal edge of teres tubercle; HTTR, teres tubercle input lever for rotation (measured at a right angle to HAR). (**D**) Anterior aspect of left radius: RL, length of radius; RDW, distal width of radius. (**E**) Lateral aspect of left ulna: UL, total length; UFL, functional length (output lever arm); UOP, length of olecranon process (input lever arm). (**F**) Posterior aspect of left ulna: UPC, width of proximal crest; ULD, least mediolateral diameter. (**G**) Posterior aspect of left femur: FL, length; FDW, distal width (epicondylar breadth); FLD, least mediolateral diameter. (**H**) Anterior aspect of left tibiofibula: TL, length; TDA, width of distal articular surface; TDW, distal width.

To assess locomotory function, we calculated 32 osteological indices (Table 1), most of which have previously been used to characterize locomotory adaptation and substrate use among soricids (Woodman and Gaffney, 2014), rodents (Price, 1993; Weisbecker and Schmid, 2007; Samuels and Van Valkenburgh, 2008; Elissamburu and De Santis, 2011) and other taxa (Lemelin, 1999; Sargis, 2002; Weisbecker and Warton, 2006; Kirk et al., 2008; Hopkins and Davis, 2009). We compared tabled indices for myosoricines with those for 1) the talpids *Uropsilus*

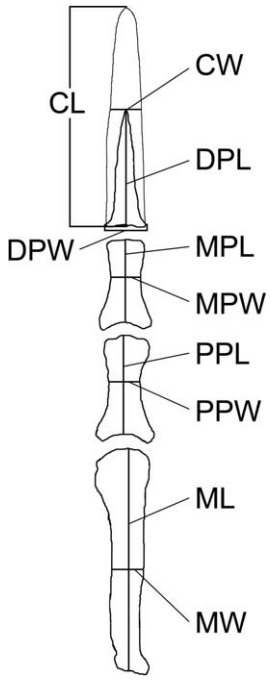

Fig. 3. Dorsal aspect of ray III of the manus illustrating variables measured on the manus and pes: ML, length of metacarpal or metatarsal; PPL, length of proximal phalanx; MPL, length of middle phalanx; DPL, length of distal phalanx; MW, width of metacarpal; PPW, width of proximal phalanx; MPW, width of middle phalanx; DPW, width of distal phalanx. An "h" preceding the abbreviation indicates the measurement derives from the pes (e.g., hMPL = length of middle phalanx of the pes).

and *Neurotrichus*, 2) two ambulatory (*Cryptotis parvus*, *C. merriami*) and one semifossorial (*C. lacertosus*) species of soricine small-eared shrews from Woodman and Gaffney (2014), and 3) summary statistics for terrestrial, semifossorial, and fossorial rodents reported by Samuels and Van Valkenburgh (2008). We also determined 1) the length of each element of the forelimb relative to the total length of the forelimb (calculated as HL + RL + ML + PPL + MPL + DPL), 2) the length of each bone of ray III of the manus relative to the total length of the ray (ML + PPL + MPL + CL), 3) the length of each element of the hind limb relative to the total length of the hind limb (FL + TL + hML + hPPL + hMPL + hDPL), and 4) the length of each bone of ray III of the pes relative to the total length of the ray (hML + hPPL + hMPL + hCL). Where data permitted, indices were calculated for each individual and summarized statistically for each species (Supporting Information Supplement 2). To account for missing data, we also calculated indices from mean values of variables (Table 2). The latter values are presented in the tables, unless otherwise stated. All indices are expressed as whole number percentages.

Of the 32 indices we investigate in our study, 10 could be calculated for only three species of myosoricines, primarily because of the lack of complete ulnae and tibiofibulae. We used two different analyses to combine the remaining 22 indices to calculate a summary score for each species. The summary scores provide an overview of interspecific variation and permit us to define relative grades of ambulatory and semifossorial adaptation. In the first analysis, we computed the percentile rank of each species for each of the 22 morphological indices (Tables 2 and 3). We then averaged the 22 percentile ranks to obtain a mean percentile rank for each species that represents its relative adaptation for ambulatory versus semifossorial locomotion on a possible scale from 0 (most ambulatory) to 100 (most semifossorial). To estimate the variance in the mean percentile ranks, we carried out a simple jackknife resampling procedure. As a further test of the stability of the scale, we recalculated mean percentile ranks using all 32 indices despite missing data (Supporting Information Supplement 3). In our second analysis, we used principal component analysis (PCA) of a covariance matrix of the same 22 indices to examine variation among myosoricines in multivariate space. We used a covariance matrix for this analysis because all indices were measured on the same 0–100 scale, so no standardization of variable scales was necessary. With the exception of the two species of *Surdisorex*, whose semifossorial behaviors are documented, our interpretations of myosoricine locomotory modes are based on these two summary scales. To ease comparisons in tables, species of myosoricines are listed in increasing order by our *a posteriori* mean percentile rank. Univariate statistics were calculated in Excel 97–2003 (Microsoft Corp., Redmond, WA) and multivariate statistics in Systat 11.00.01 (Systat Software, Chicago, IL).

RESULTS

Mean Percentile Ranks

Within a possible range from 0 (most ambulatory) to 100 (most semifossorial), the mean percentile ranks for myosoricines range from 18 to 83 (Table 3; Fig. 4). Mean percentile ranks for the ambulatory talpid *Uropsilus* (33) and the semifossorial talpid *Neurotrichus* (75) provide a general guide for this scale. Standard deviations for mean percentile ranks, calculated from jackknife resampling, range from 0.4 to 1.1 among the myosoricines, but are higher for the two moles. The relative order of myosoricine species remained the same for each iteration of the jackknife procedure. When we calculated percentile ranks for all 32 indices, the order of these species also remained the same (Supporting Information Supplement 3), indicating some degree of stability in our sample. The addition or subtraction of taxa used in the calculations could change the mean rankings substantially, however, so they are only meaningful within the context of our study.

Based on the distribution of mean percentile rankings, the most ambulatory myosoricine among the nine species we examined is *M. cafer*, and the most semifossorial is *S. norae*. The average difference in rankings between adjacent myosoricine species on this scale is eight percentile points (Table 3). Differences >8 percentile points between adjacent species occur in only two places. At the lower end of the scale, *M. cafer* is separated from *M. geata* by 12 percentile points, and on the higher end of the scale, *M. zinki* is separated from *S polulus* by 16 percentile points. As a comparison, the mean percentile ranking for *Uropsilus* places the ambulatory mole between *M. kihaulei* and *C. phillipsorum*. This suggests that *M. cafer*, *M. geata*, and *M. kihaulei* are more suited to ambulatory locomotion than other myosoricines. The semifossorial *Neurotrichus* ranks above *M. zinki* and below *S. polulus* and *S. norae*, which suggests that the two species of *Surdisorex* are more adapted for digging than *Neurotrichus*.

TABLE 1. List of indices used in this study, with their abbreviations in parentheses

1. Intermembral index (IM = [HL + RL]/[FL + TL]) compares the lengths of the forelimbs and hind limbs (Sargis, 2002). IM typically increases with increasing fossoriality in rodents (Samuels and Van Valkenburgh, 2008).
2. Humerofemoral index (HFI = HL/FL) represents the length of the humerus as a proportion of the length of the femur (Sargis, 2002).
3. Metapodial index (FOOT = ML/hML) indicates the relative sizes of the forefeet and hind feet by comparing the length of metacarpal III to that of metatarsal III.
4. Distal phalanx length index (CLAW = DPL/hDPL) compares the relative size of distal phalanx III of the manus to distal phalanx III of the pes. It increases with increasing fossoriality in rodents (Samuels and Van Valkenburgh, 2008).
5. Claw length index (CLI = CL/hCL) gauges the relative size of claw III of the manus to claw III of the pes.
6. Scapulohumeral index (SHI = SL/HL) indicates relative lengths of the scapula and humerus. This index is typically greater for more semifossorial eulipotyphlans (Woodman and Gaffney, 2014).
7. Brachial index (BI = RL/HL) shows the relative proportions of the proximal (humerus) and distal (radius) elements of the forelimb. The index decreases with increasing fossoriality among rodents (Samuels and Van Valkenburgh, 2008).
8. Shoulder moment index (SMI = HDPC/HL) gauges the size and mechanical advantage of the deltoid and pectoral muscle groups, which are important in the movement, rotation, and counter-rotation of the humerus (Reed, 1951), by comparing the length of the deltopectoral crest, on which these muscles insert, to the length of the humerus. This is the same as the delto-pectoral crest length index (Sargis, 2002). The index increases with increasing fossoriality among rodents (Samuels and Van Valkenburgh, 2008).
9. Humeral robustness index (HRI = HLD/HL) indicates the robustness of the humerus and its ability to resist bending and shearing stresses. The index increases with increasing fossoriality among rodents (Samuels and Van Valkenburgh, 2008).
10. Humeral rotation lever index (HTI = HTTR/HAR) shows the relative length of the teres tubercle measured at right angles to the longitudinal axis of rotation of the humerus. The teres tubercle is an elongate process on the eulipotyphlan humerus that serves as the insertion for the large latissimus dorsi and teres major muscles and as a lever for rotating the humerus (Reed, 1951). HTI increases with increased semifossoriality among species of *Cryptotis* (Woodman and Gaffney, 2014).
11. Teres tubercle position index (TTP = HTT/HAR) represents the relative position of the teres tubercle along the axis of rotation of the humerus (HAR). In more robust humeri with larger surfaces for muscle attachment, the teres tubercle is often more distally positioned. Hence, the index should increase with greater semifossoriality.
12. Humeral epicondylar index (HEB = HDW/HL) measures the width of the distal humerus relative to the length of the humerus and represents the area available for the origins of muscles involved in flexing, pronating, and supinating the forearm. It typically increases in mammals with increasing semifossoriality and fossoriality (Hildebrand, 1985b; Samuels and Van Valkenburgh, 2008).
13. Radial distal width index (RDW = RDW/RL) measures the relative width of the distal end of the radius, providing a gauge of its robustness and its resistance to the stresses associated with digging.
14. Olecranon length index (OLI = UOP/UFL) is one of many variations on the index of fossorial ability of Hildebrand (1985a). The ulna acts as a lever that pivots at the trochlear notch, and OLI is used to gauge the amount of force exerted by the triceps brachii muscle on the olecranon process that is transmitted to the functional arm of the ulna. More semifossorial and fossorial mammals generally have a longer olecranon process to accommodate a larger triceps brachii, resulting in larger OLI (Reed, 1951; Vizcaino and Milne, 2002; Samuels and Van Valkenburgh, 2008; Woodman and Gaffney, 2014).
15. Triceps metacarpal outforce index (TMO = UOP/[UFL + ML]) gives the length of the olecranon process as a proportion of the functional arm provided by the ulna and metacarpal III. A variation of OLI, this index measures the amount of force input on the olecranon process that is transmitted to the tip of the metacarpal of ray III (Price, 1993).
16. Triceps claw outforce index (TCO = UOP/[UFL + ML + PPL + MPL + CL]) expresses the length of the olecranon process relative to the combined functional lengths of the ulna and ray III. An extension of Hildebrand's (1985a) index of fossorial ability and Price's (1993) triceps metacarpal outforce index, TCO represents the proportion of force input on the olecranon process by the triceps muscle that is transmitted to the tip of the claw of ray III, which is the initial point of contact with the soil.
17. Olecranon crest index (OCI = UPC/UFL) is a measure of the relative length of the olecranon crest, a prominent structure on the olecranon process of many eulipotyphlans, which is the insertion for much of the triceps brachii. OCI is an approximate gauge of muscle size, and, therefore, another measure of the relative input force on the ulna (Woodman and Gaffney, 2014).
18. Ulnar robustness index (URI = ULD/UFL) measures the robustness of the ulna and its ability to resist bending and shearing stresses. URI increases with semifossoriality and fossoriality (Samuels and Van Valkenburgh, 2008).
19. Relative length of the manual distal phalanx [%DPL = DPL/(ML + PPL + MPL)] is the length of distal phalanx III of the manus relative to the combined length of the proximal three bones of ray III.
20. Relative length of the manual claw [%CL = CL/(ML + PPL + MPL)] is the length of claw III of the manus relative to the combined length of the proximal three bones of ray III.
21. Relative support for the claw (%CLS = DPL/CL) represents the proportion of claw III of the manus that is supported by distal phalanx III.
22. Metacarpal width index (MW3 = MW/ML) measures the robustness of metacarpal III of the manus in relation to its length.
23. Phalangeal index (PI = (PPL + MPL)/ML) shows the lengths of the proximal and middle phalanges relative to the metacarpal. The index varies considerably among rays of an individual, so ray III is typically used for comparisons among species (Lemelin, 1999).
24. Manus proportions index (MANUS = PPL/ML) measures the size of the proximal phalanx relative to the metacarpal (Kirk et al., 2008; Samuels and Van Valkenburgh, 2008). This is the same as Kirk et al.'s (2008) proximal phalangeal index.
25. Crural index (CI = TL/FL) measures the relative lengths of proximal (femur) and distal (tibiofibula) long bones of the hind limb. Like the brachial index, this decreases with increasing fossoriality among rodents (Samuels and Van Valkenburgh, 2008).
26. Pes length index (PES = hML/FL) represents the length of metatarsal III relative to femur length and has been used to indicate the relative size of the hind foot (Samuels and Van Valkenburgh, 2008).
27. Femoral robustness index (FRI = FLD/FL) quantifies the robustness of the femur and its ability to resist bending and shearing stresses.
28. Femoral epicondylar index (FEB = FDW/FL) approximates the area available for the origins of the gastrocnemius and soleus muscles used in extension of the knee and plantar-flexion of the pes in rodents (Samuels and Van Valkenburgh, 2008). In shrews and talpids, the same region is the origin for the plantaris (toe flexor), gastrocnemius (pes extensor), extensor digitorum longus (extensor and adductor of digits; dorsoflexor of foot), and insertion for the caudofemoralis (femur retractor) and adductor longis (femur adductor; Reed, 1951).
29. Distal tibiofibular articulation index (DTA = TDA/TDW) measures the width of the articular region for the astragalus between the lateral and medial malleolus relative to the distal width of the tibia.
30. Relative length of the pedal distal phalanx [%hDPL = hDPL/(hML + hPPL + hMPL)] is the length of the distal phalanx of ray III of the pes relative to the combined length of the proximal three bones of that ray.
31. Relative length of the pedal claw [%hCL = hCL/(hML + hPPL + hMPL)] is the length of the claw of ray III of the pes relative to the combined length of the proximal three bones of that ray.
32. Relative support for the pedal claw (%hCLS = hDPL/hCL) is the proportion of the claw of ray III of the pes supported by the distal phalanx.

All indices are expressed as whole number percentages.

TABLE 2. Mean indices calculated for myosoricines

	IM	HFI	FOOT	CLAW	CLI	SHI	BI	SMI	HRI	HTI	TTP
M. cafer	—	88	71	100	114	92	—	46	10	15	36
M. geata	—	91	72	93	116	94	—	47	9	16	39
M. kihaulei	—	90	70	97	117	94	—	46	9	16	40
C. phillipsorum	—	90	76	113	107	104	—	50	11	20	39
M. varius	70	86	69	109	126	99	103	48	10	18	43
M. blarina	72	89	77	107	128	100	96	50	9	19	41
M. zinki	—	82	75	120	152	108	—	47	13	18	42
S. polulus	—	84	79	162	174	113	—	62	17	39	55
S. norae	70	81	71	143	166	120	103	62	17	35	51
Soricines											
C. parvus	71	86	66	97	103	100	103	42	9	17	40
C. merriami	73	92	68	99	96	95	93	44	9	17	38
C. lacertosus	75	92	67	125	131	123	102	44	15	33	51
Talpids											
U. soricipes	70	88	54	81	88	125	128	44	10	16	39
N. gibbsii	66	82	41	123	123	174	119	62	22	38	50
Rodents											
Terrestrial	74	—	—	79	—	—	100	42	9	—	—
Semifossorial	76	—	—	116	—	—	92	46	10	—	—
Fossorial	85	—	—	159	—	—	91	54	11	—	—

	HEB	RDW	OLI	TMO	TCO	OCI	URI	%DPL	%CL	%CLS	MW3
M. cafer	32	—	—	—	—	—	—	19	36	51	11
M. geata	35	—	—	—	—	—	—	21	42	50	13
M. kihaulei	35	—	—	—	—	—	—	23	46	49	12
C. phillipsorum	42	—	—	—	—	—	—	23	39	59	13
M. varius	35	13	19	14	10	30	5	27	52	52	14
M. blarina	39	15	24	18	12	31	8	28	57	49	15
M. zinki	47	—	—	—	—	—	—	29	61	48	16
S. polulus	58	—	—	—	—	—	—	45	76	59	20
S. norae	60	17	31	23	14	40	9	46	78	60	20
Soricines											
C. parvus	36	13	18	13	9	24	6	16	35	46	10
C. merriami	35	12	20	15	11	27	7	15	29	52	10
C. lacertosus	58	17	28	21	14	40	9	36	63	58	20
Talpids											
U. soricipes	44	9	16	12	8	17	4	22	40	55	12
N. gibbsii	54	19	26	21	13	36	7	68	104	65	41
Rodents											
Terrestrial	25	—	16	—	—	—	4	—	—	—	—
Semifossorial	29	—	22	—	—	—	6	—	—	—	—
Fossorial	37	—	33	—	—	—	7	—	—	—	—

	PI	MANUS	CI	PES	FRI	FEB	DTA	%HDPL	%HCL	%HCLS
M. cafer	91	55	—	48	8	21	—	15	26	58
M. geata	90	54	—	46	10	23	—	19	31	62
M. kihaulei	88	53	—	47	10	23	—	19	32	59
C. phillipsorum	87	55	—	46	10	24	—	18	32	56
M. varius	88	52	149	44	9	22	45	20	34	60
M. blarina	84	50	142	40	10	24	46	23	39	59
M. zinki	86	51	—	42	11	25	—	21	34	60
S. polulus	83	49	—	42	10	24	—	25	39	64
S. norae	84	50	135	42	11	25	44	27	38	69
Soricines										
C. parvus	96	58	145	46	8	23	41	13	26	49
C. merriami	98	62	143	44	10	22	43	12	23	50
C. lacertosus	97	58	147	41	10	28	48	23	38	60
Talpids										
U. soricipes	104	66	186	60	9	26	50	18	30	60
N. gibbsii	135	81	169	50	10	27	46	30	46	65
Rodents										
Terrestrial	—	62	119	50	8	18	—	—	—	—
Semifossorial	—	58	109	41	9	21	—	—	—	—
Fossorial	—	52	105	36	10	25	—	—	—	—

Comparable values for soricines and rodents are from Woodman and Gaffney (2014) and Samuels and Van Valkenburgh (2008), respectively. Abbreviations explained in Table 1.

TABLE 3. Percentile ranks for the 22 indices used to calculate the mean percentile rank (mean rank) for each taxon

	HFI	FOOT	CLAW	CLI	SHI	SMI	HRI	HTI	TTP	HEB	% DPL	%CL	% CLS
M. cafer	45	55	32	23	5	18	41	5	5	5	5	5	41
M. geata	5	41	14	32	18	36	14	23	23	23	14	32	32
M. kihaulei	18	68	23	41	18	18	14	23	41	23	36	41	18
C. phillipsorum	18	23	59	14	50	64	59	68	23	50	36	14	72
M. varius	59	77	50	59	32	50	41	45	68	23	50	50	50
M. blarina	32	14	41	68	41	64	14	59	50	41	59	59	18
M. zinki	81	32	68	77	59	36	68	45	59	68	68	68	5
S. polulus	68	5	95	95	68	86	82	95	95	86	77	77	72
S. norae	95	55	86	86	77	86	82	77	86	95	86	86	86
U. soricipes	45	86	5	5	86	5	41	23	23	59	23	23	59
N. gibbsii	81	95	77	50	95	86	95	86	77	77	95	95	95

	MW3	PI	MANUS	PES	FRI	FEB	%HDPL	%HCL	%HCLS	Sum	Mean Rank	SD
M. cafer	5	23	27	23	5	5	5	5	14	397	18	±0.8
M. geata	36	32	41	45	54	27	36	23	68	669	30	±0.7
M. kihaulei	18	45	50	32	54	27	36	36	27	707	32	±0.7
C. phillipsorum	36	59	27	45	54	50	18	36	5	880	40	±0.9
M. varius	50	45	59	59	18	14	50	55	50	1054	48	±0.7
M. blarina	59	81	82	95	54	50	68	81	27	1157	53	±1.1
M. zinki	68	68	68	77	91	73	59	55	50	1343	61	±0.9
S. polulus	82	95	95	77	54	50	77	82	77	1690	77	±1.0
S. norae	82	81	82	77	91	73	86	68	95	1818	83	±0.4
U. soricipes	18	14	14	5	18	86	18	14	50	720	33	±1.3
N. gibbsii	95	5	5	14	54	95	95	95	86	1648	75	±1.4

Abbreviations of indices are explained in Table 1. Standard deviation (SD) of mean percentile rank is from jackknife resampling. See also Supporting Information Supplement 3.

Principal Component Analysis

The first four principal components (PCs) from our PCA all have eigenvalues >1,000 (Table 4). Most indices have high positive loadings on PC1, which explains >59% of the variation in the model. One exception is the index FOOT, which has a low negative loading on this component. PC2 is mostly a contrast between FOOT and the three indices PES, MANUS, and PI. It explains >19% of the variation and distinguishes *M. blarina* (low negative score) and the two talpids (high positive scores) from the other eight species based on the relative lengths of their metapodials and phalanges. A plot of factor scores on these two components is shown in Figure 5. PC3 (not shown) is a contrast between FOOT and %CLS. It

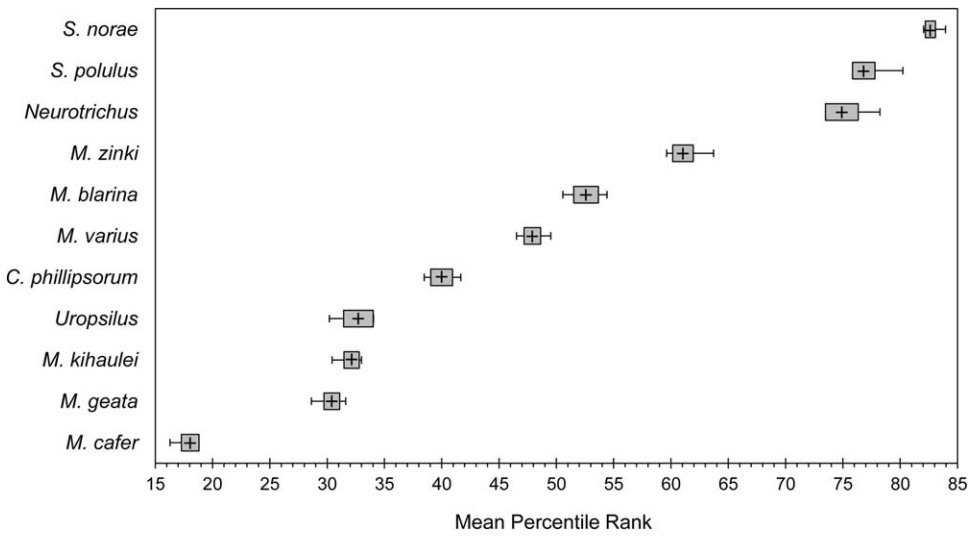

Fig. 4. Boxplots of mean percentile ranks for each species. Mean (crosses), SD (boxes), and range (whiskers) are from jackknifed resampling (Table 3).

TABLE 4. Component loadings and eigenvalues from PCA of covariance matrix of 22 morphological indices (see Fig. 5)

Variable	PC1	PC2	PC3	PC4
MW3	28.995	1.291	1.794	1.223
DPL	28.868	2.504	2.897	0.154
HDPL	27.848	0.165	8.18	2.002
CL	27.797	1.614	9.949	0.178
TTP	27.65	−1.652	5.917	5.013
HTI	26.729	1.031	−10.025	3.459
HCL	26.677	−2.136	2.655	4.142
CLAW	26.654	−2.142	−7.462	6.209
HEB	25.737	7.152	−5.578	−9.791
SMI	25.552	−1.559	−8.39	8.866
CLI	24.639	−13.789	7.745	2.582
HFI	22.631	7.8	5.768	0.842
HRI	22.15	12.59	−8.077	2.19
HCLS	21.076	8.986	10.591	0.722
SHI	20.644	17.098	−4.121	−10.049
FRI	18.135	−7.118	0.94	−13.356
FEB	17.323	15.982	−1.945	−17.054
PES	15.771	−23.769	−0.081	−2.215
PI	15.755	−22.774	−6.911	−3.596
MANUS	15.291	−23.778	3.439	−0.559
CLS	13.875	18.455	−12.458	10.399
FOOT	−5.774	23.522	14.393	4.789
Eigenvalues	11,504.461	3,708.648	1,191.546	1,004.96
Total variance explained (%)	59.667	19.235	6.18	5.212

Abbreviations of variables are explained in Figures 2 and 3.

explains >6% of the variation and effectively separates *C. phillipsorum* (low negative score) from the other 10 species based on its relatively short claws and long distal phalanges. PC4 (not shown) explains >5% of the variation and is most influenced by FRI and FEB. This component separates *Uropsilus* and *M. zinki* (low negative scores) and *M. cafer* and *M. varius* (high positive scores) from the remaining seven species based on the relative robustness of their femurs.

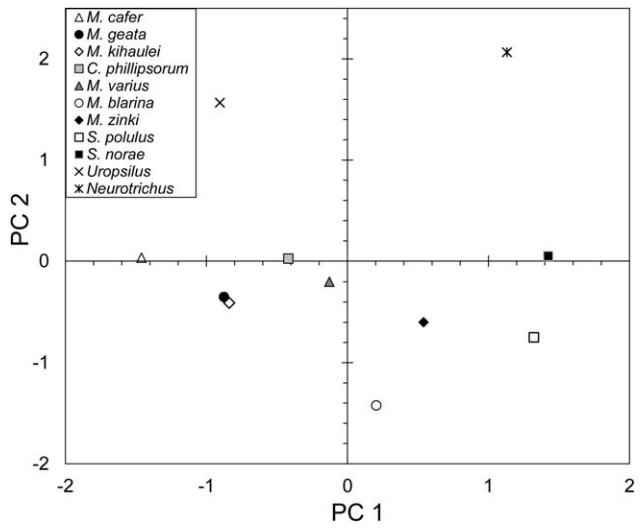

Fig. 5. Plot of factor scores on the first two PCs from PCA of 22 indices from nine myosoricines and two talpids. PC1 accounts for >59% of the variance; PC2 for >19% (see Tables 4 and 5).

PC1 incorporates 21 of the 22 indices and effectively describes a locomotory gradient from more ambulatory (more negative) to more semifossorial (more positive). The individual scores on PC1 (Table 5) provide a convenient means of ranking the locomotory ability of each species in the analysis. This ranking presents the same order of species as that provided by the mean percentile rankings (Table 3). The average difference in scores between adjacent myosoricine species on this scale is 0.362 (Table 5). Differences in adjacent scores greater than that value occur at three places, two of which are the same as the large gaps in the scale of mean percentile rankings: *M. cafer* is separated from *M. geata* by 0.595, *M. kihaulei* is separated from *C. phillipsorum* by 0.421, and *M. zinki* is separated from *S. polulus* by 0.769. The talpid *Neurotrichus* scores between *M. zinki* and *S. polulus*, which is the same relative position it had for the mean percentile rankings. The score for the ambulatory mole *Uropsilus*, however, places it between *M. cafer* and *M. geata*, which is lower on the scale compared to its position based on mean percentile rankings. The order of species on the PC1 scale suggests that only *M. cafer* is more suited to ambulatory locomotion than *Uropsilus*.

DISCUSSION

Morphological Variation Related to Locomotory Mode

We used the scale from our mean percentile ranks analysis as our primary model of relative locomotory mode in myosoricines. By understanding variation in the relative proportions of elements of the limbs (Tables 6 and 7) and the performance of each of the 32 indices (Table 2) in the context of this model, we reconstructed general patterns of variation in the myosoricine postcranial skeleton as they relate to locomotory function. In the following discussions, more ambulatory species are considered to be those that had lower

TABLE 5. Rounded factor scores on PC1 (see Fig. 5)

Species	PC1 Score
M. cafer	−1.46
M. geata	−0.87
M. kihaulei	−0.84
C. phillipsorum	−0.42
M. varius	−0.13
M. blarina	0.20
M. zinki	0.54
S. polulus	1.32
S. norae	1.42
U. soricipes	−0.90
N. gibbsii	1.13

TABLE 6. Proportional contribution of the bones of the forelimb and hind limbs relative to their respective total lengths, calculated from mean values

	Forelimb length								
	Mean (mm)	% HB	Humerus	Radius	Metacarpal	Proximal phalanx	Middle phalanx	Distal phalanx	Claw
Myosorex varius	27.3	32	35	36	12	6	4	6	12
Myosorex blarina	27.3	37	36	35	12	6	4	6	13
Surdisorex norae	30.6	35	33	34	12	6	4	10	17
Cryptotis parvus	17.5	30	35	36	12	7	5	4	8
C. merriami	20.7	30	37	35	12	7	4	4	7
C. lacertosus	24.9	30	34	36	12	7	4	8	13
U. soricipes	25.4	36	31	40	11	7	4	5	9
N. gibbsii	21.5	31	31	37	8	6	4	13	19
	Hind limb length								
	Mean (mm)	% HB	Femur	Tibia	Metatarsal	Proximal phalanx	Middle phalanx	Distal phalanx	Claw
Myosorex varius	36.9	44	30	45	13	5	3	4	7
Myosorex blarina	35.6	48	31	44	12	5	3	5	8
Surdisorex norae	40.0	46	31	42	13	5	3	6	8
Cryptotis parvus	24.0	41	30	44	14	6	3	3	6
C. merriami	27.8	40	31	44	13	6	3	3	5
C. lacertosus	31.7	39	30	44	12	5	3	5	8
U. soricipes	36.3	51	25	46	15	7	3	4	7
N. gibbsii	31.8	45	26	44	13	7	3	7	11

Comparable values for *Cryptotis* are from Woodman and Gaffney (2014). Except for mean forelimb length and mean hind limb length (mm), all numbers are percentages. %HB is limb length as a proportion of the head-and-body length.

TABLE 7. Mean lengths of individual elements of ray III of the manus and pes relative to the total length of the ray including the claw

	Metacarpal/ Metatarsal	Proximal phalanx	Middle phalanx	Distal phalanx	Claw
Manus					
M. cafer	38	21	14	14	27
M. geata	37	20	13	15	30
M. kihaulei	36	19	13	15	31
C. phillipsorum	38	21	12	17	28
M. varius	35	18	13	18	34
M. blarina	35	17	12	18	36
M. zinki	34	17	12	18	38
S. polulus	31	15	11	26	43
S. norae	31	15	10	26	44
Cryptotis parvus	38	22	14	12	26
C. merriami	37	23	13	11	21
C. lacertosus	31	18	12	22	39
U. soricipes	35	23	13	16	29
N. gibbsii	21	17	11	33	51
Pes					
M. cafer	48	20	12	12	21
M. geata	47	18	11	15	24
M. kihaulei	47	18	11	14	24
C. phillipsorum	46	19	10	14	24
M. varius	47	18	10	15	25
M. blarina	44	17	11	17	28
M. zinki	46	18	11	15	25
S. polulus	44	18	10	18	28
S. norae	43	18	10	20	29
C. parvus	47	20	11	10	20
C. merriami	47	22	12	9	19
C. lacertosus	44	18	11	17	27
U. soricipes	42	22	11	15	26
N. gibbsii	38	21	10	21	32

Values for *Cryptotis* are from Woodman and Gaffney (2014). All numbers are percentages.

scores on the scale of mean percentile ranks; more semifossorial species had higher scores.

Forelimb versus hind limb. Adaptations for fossoriality in mammals can include reductions in the overall lengths of the limbs, with the hind limbs shortening at a greater rate than the forelimbs (Shimer, 1903; Samuels and Van Valkenburgh, 2008). This does not appear to be the general pattern in mysoricines, which show no clear trend (Table 2: IM, HFI, FOOT; Table 6). Moreover, the myosoricine humerus typically becomes shorter relative to the femur (HFI) in more semifossorial species, a pattern that is also seen in talpids (Reed, 1951).

Scratch-digging fossorial mammals typically have measurably enlarged foreclaws and underlying distal phalanges (Hildebrand, 1985b). The hind claws also are generally larger but not to the same extent as the foreclaws (Shimer, 1903; Reed, 1951). This pattern holds for myosoricines as well (Table 2: CLAW, CLI).

Forelimb. Unlike rodents (Samuels and Van Valkenburgh, 2008) and talpids (Table 6), there is no clear pattern of forelimb reduction among the few myosoricines for which we could obtain complete measurements. Although the humerus and radius may shorten slightly, the proportional lengths of many of the bones contributing to the forelimb are remarkably stable both in myosoricines and soricines (Table 6). The most variable elements are the claw and the distal phalanx, which, as noted previously, increase in length with increasing semifossoriality.

Scapula. Reed (1951) described the elongation of the scapula among semifossorial and fossorial talpids. More semifossorial species of myosoricines also have longer scapulae than more ambulatory species (Table 2: SHI). One exception is *C. phillipsorum*, which has a longer scapula than would be expected based on its mean percentile ranking.

Humerus. The radius becomes shorter relative to the humerus in more fossorial rodents and talpids (Samuels and Van Valkenburgh, 2008). No such pattern emerged among myosoricines or soricines (Table 2: BI; Table 6).

The length of the deltopectoral crest of the humerus increases with increasing semifossoriality among rodents and talpids (Table 2: SMI) as the size and power of the deltoid and pectoral muscles increase (Samuels and Van Valkenburgh, 2008). With the exception of *C. phillipsorum*, which has a long crest for a short-clawed shrew, myosoricines exhibit a similar pattern of lengthening deltopectoral crest with increasing semifossoriality.

Among mammals, it is common for more semifossorial species to have more robust limb bones, including humeri (Hildebrand, 1985b; Samuels and Van Valkenburgh, 2008; Woodman and Gaffney, 2014). With the exception of *C. phillipsorum*, which has a more robust humerus than expected based on its mean percentile rank, the humerus increases in breadth with increasing semifossoriality among myosoricines (Table 2: HRI).

In soricines, the teres tubercle is visibly longer (Table 2: HTI) and more distally positioned along the humerus (TTP) with increasing semifossoriality (Fig. 1; Woodman and Gaffney, 2014). With the exception of *C. phillipsorum*, which has an unexpectedly long tubercle, both indices increase with increasing semifossoriality among myosoricines.

The relative breadth of the distal end of the humerus typically increases with increasing semifossoriality among mammals (Hildebrand, 1985b), and this is the pattern among myosoricines (Table 2: HEB), with the exception of *C. phillipsorum*, which has a broader distal end of the humerus than expected.

Radius. The mammalian radius is generally more robust in more semifossorial species, and there is a similar pattern among the few myosoricines for which radii were available to measure (Table 2: RDW).

Ulna. Semifossorial and fossorial mammals generally have a longer olecranon process and a shorter functional arm of the ulna, resulting in greater force being transmitted. This increase in force is indicated by larger OLI, TMO, TCO, and OCI (Reed, 1951; Price, 1993; Samuels and Van Valkenburgh, 2008; Woodman and Gaffney, 2014). We had only three species of myosoricines with complete ulnae, but they exhibited an increase in all four indices with increasing semifossoriality (Table 2). *Surdisorex norae* is notable because it has a higher mean OLI than those calculated for soricine shrews, semifossorial rodents, and the semifossorial mole *Neurotrichus*, suggesting that it can bring more power to bear when digging than any of those other mammals.

As with other bones of the forelimb, the mammalian ulna increases in robustness with increasing semifossoriality and fossoriality, and this pattern holds for myosoricines (Table 2: URI).

Manus. Among myosoricines, distal phalanges (%DPL) and claws of the manus (%CL; Tables 2 and 7; Fig. 6) increase in length with increased semifossoriality. The distal phalanx lengthens at a faster rate than the claw (%CLS), which provides more semifossorial species with greater underlying support for the claw (Woodman and Gaffney, 2014; Woodman and Stabile, 2015). An exception is *C. phillipsorum*, which has a relatively short claw, but a long distal phalanx, resulting in a higher measure of support than would be expected based on the claws and the distal phalanges of other mysoricines.

In contrast to the distal phalanges and claws, the metacarpals and proximal and middle phalanges shorten with increasing semifossoriality

(Table 7; Fig. 6A). Moreover, the proximal and middle phalanges shorten at a higher rate than the metacarpal, resulting in decreases in the indices PI and MANUS (Table 2). This is opposite of the trend in talpids, in which the metacarpal shortens much more than the proximal and middle phalanges with increasing semifossoriality (Table 2; Reed, 1951). As in other groups of mammals (Hildebrand, 1985b), the breadths of the bones of the manus (MW3) increase with increasing semifossoriality in myosoricines.

Hind limb. Like the forelimb, there is no clear pattern of hind limb reduction or increase with locomotory mode among the few myosoricines for which we could obtain complete measurements (Table 6). The proportional lengths of most individual elements of the hind limb remain relatively stable, although the tibiofibula (CI; Table 2) and metatarsal III (PES) exhibit some shortening relative to the femur with increased semifossoriality, a pattern also seen in rodents (Samuels and Van Valkenburgh, 2008). The most variable elements are the claw and the distal phalanx, which increase in length with increasing semifossoriality, but the increases are much lower in magnitude than for the same elements of the forelimb.

Femur. As for other groups of mammals (Samuels and Van Valkenburgh, 2008; Woodman and Gaffney, 2014; Table 2), the breadths of the diaphysis (Table 2: FRI) and the distal end of the femur (FEB) generally increase with increasing semifossoriality among myosoricines.

Tibiofibula. The breadth of the distal tibiofibular articulation with the astragalus shows no clear pattern among myosoricines (Table 2: DTA), unlike in talpids and soricines (Woodman and Gaffney, 2014).

Pes. In general, morphological changes in the bones of the myosoricine pes mirror those for the manus but at lower magnitude. The metatarsals and proximal and middle phalanges generally shorten with increasing semifossoriality (Fig. 6B), whereas distal phalanges (%hDPL) and claws (%hCL) lengthen (Table 7). The distal phalanx increases in length at a faster rate than the claw (%hCLS), thereby providing greater support for the claw in more semifossorial species. An exception is *M. zinki*, which has a longer metatarsal and shorter distal phalanx and claw than expected based on the relative lengths of these elements on the forefoot (Fig. 6B).

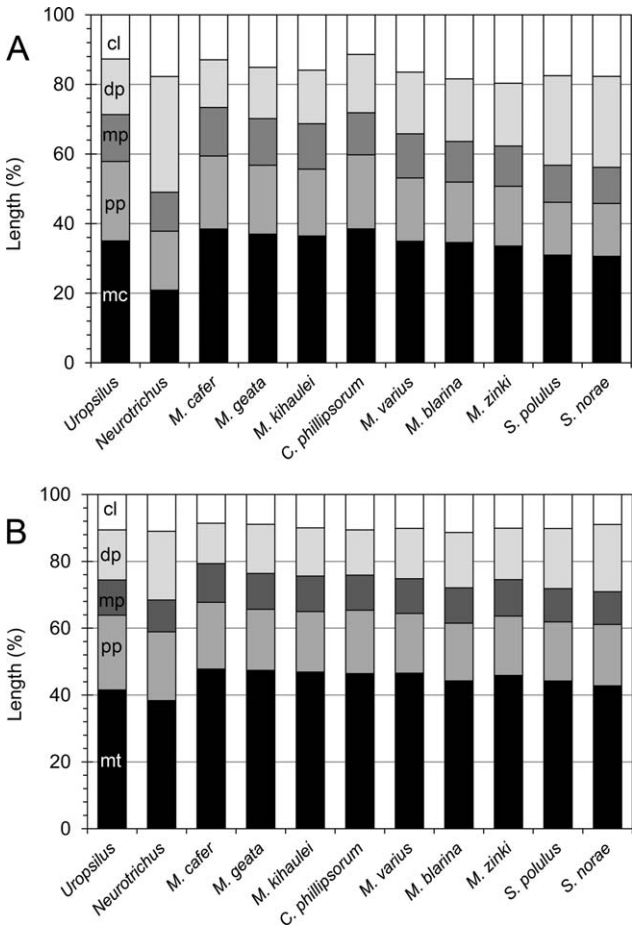

Fig. 6. Plots of (**A**) mean proportional lengths of the metacarpal (mc), proximal phalanx (pp), middle phalanx (mp), distal phalanx (dp), and protruding claw (cl) of ray III of the manus; and (**B**) mean proportional lengths of the metatarsal (mt), proximal phalanx (pp), middle phalanx (mp), distal phalanx (dp), and protruding claw (cl) of ray III of the pes. Lengths of individual bones and claws are relative to the complete length of the ray including the claw. The protruding claw is that part of the claw that extends beyond the tip of the distal phalanx.

General Morphological Trends

Morphological variation associated with locomotory behavior in myosoricines takes the form of a graded series in which individual elements of the skeleton lengthen or shorten and become more robust with greater adaptation for semifossoriality. In summarizing this variation, we treated the variation as a continuum and addressed changes in morphology as a unidirectional transition from ambulatory to semifossorial. No complete phylogeny for the Myosoricinae currently exists, so it is difficult to understand locomotory adaptations within a true evolutionary framework. Regardless, it is important to keep in mind that rather than representing a single lineage sampled at discrete intervals, the variation we describe is present at the extant tips of genetically divergent lineages, each of which has some period of independent evolutionary history (Quérouil et al., 2001; Willows-Munro and Matthee, 2009, 2011). The discrete morphological gradation we document suggests that adaptation overrides phylogeny in our

dataset. If this proves to be so, it would indicate that the appearance of gradation is illusory. Because selection for ambulatory behavior is as likely as selection for semifossorial behavior, it is also important to consider that evolution may occur in either direction.

In evolving toward a more fossorial mode of life, myosoricines exhibit a number of morphological changes that are typical adaptations for scratch-digging mammals (Shimer, 1903; Reed, 1951; Hildebrand, 1985b; Samuels and Van Valkenburgh, 2008; Woodman and Gaffney, 2014). The claws and underlying distal phalanges of the manus and pes increase in length and breadth, while the metacarpals, metatarsals, and proximal and middle phalanges shorten and broaden. These changes are more obvious on the forefoot than on the hind foot. The diaphyses of the humerus, radius, ulna, and femur become more robust, and regions of the bones involved in the origin and insertion of forelimb extensor and flexor muscles increase in size, resulting in enlarged bony processes. The olecranon process of the ulna increases in length relative to the distal functional arm.

Myosoricines also show morphological changes that are unique to eulipotyphlans, soricids, and their own subfamilial clade. Adaptations for semifossoriality and fossoriality often include reductions in the lengths of the limbs (Shimer, 1903), as occurs in rodents and moles (Reed, 1951; Samuels and Van Valkenburgh, 2008). A shorter forelimb is a consequence of shortening of the antebrachium to deliver greater leverage in digging, while a shorter hind limb results from shortening of the tibiofibula and hind foot. Shortening of the hind limb is typically greater than shortening of the forelimb (Samuels and Van Valkenburgh, 2008). Yet, there is no evidence for limb shortening in myosoricines or other soricids. This absence does not, however, translate as complete stasis in pectoral girdle. The myosoricine scapula generally increases in length with increasing semifossoriality (as in other soricids and talpids), and there are modest decreases in the lengths of humerus and radius (as in talpids). Like other groups of mammals, increased fossoriality in myosoricines is tied to noticeable changes in the morphology of the humerus; it becomes more robust, the deltopectoral crest elongates, and the medial and lateral epicondyles enlarge. In contrast to soricines, in which the deltopectoral crest is less pronounced proximally and is offset toward the lesser tuberosity (Reed, 1951; Woodman and Gaffney, 2014), in myosoricines the crest forms a continuous ridge that extends proximally to the greater tuberosity. Although these differences were not quantified, the myosoricine humerus also has a more prominent trochlea and a longer medial epicondyle than in soricines (compare to Reed, 1951; Woodman and Gaffney, 2014), two characteristics also present in some lower Miocene myosoricines (Klietmann et al., 2014:Fig. 6). A teres tubercle is a feature of the humerus unique to talpids, soricids, tachyglossids, and a few early mammals (Hildebrand, 1985b; Martin, 2005; Woodman and Gaffney, 2014). As in other soricids, this process increases in size and becomes more distally positioned with increasing semifossoriality, and it suggests that, like talpids, some degree of humeral rotation is involved in the digging stroke (Reed, 1951; Woodman and Gaffney, 2014).

The unique and variable morphologies of the myosoricine skeleton allow for predictions about digging adaptations and point toward an ecological radiation in behavior and substrate use. How the sometimes subtle variation in morphology may be affected by soil composition, prey availability, predation risk, and other ecological factors remains to be determined.

Congosorex phillipsorum

Congosorex phillipsorum is distinctive among modern Myosoricinae because it possesses a seemingly contradictory combination of ambulatory and semifossorial characteristics. The species has comparatively short claws, the bones of the manus are not particularly broad, and it ranks relatively low on both the mean percentile ranks and PC1 scales, suggesting that it is a more ambulatory species. Yet, a number of individual characters point toward a more semifossorial mode. It possesses a longer scapula than would be expected for an ambulatory species and the processes of the humerus are more developed. These latter include a long (but not more distally positioned) teres tubercle, broad lateral and medial epicondyles, and long deltopectoral crest (Fig. 1). The diaphysis of the humerus (but not the diaphysis of the femur) is also more robust than would be expected for an ambulatory species. Although it bears short claws on its forefeet, *C. phillipsorum* has moderately long distal phalanges, resulting in a higher measure of support for the claws than would be expected based on the claws and distal phalanges of other myosoricines. In contrast, the hind feet of *C. phillipsorum* have moderately long claws and short distal phalanges, resulting in a low level of support for the claws. Overall, the skeletal characteristics of *C. phillipsorum* suggest a unique, but enigmatic, functional mode for this species. The robust humerus has relatively strong muscle attachment regions, but it is not obvious how the relatively slender bones of manus would bear the force generated by those muscles (Woodman and Stabile, 2015). The claws are

well-supported but short, suggesting either that *C. phillipsorum* excavates in a novel substrate or that its primary activity is not typical scratch-digging. Unfortunately, a number of potentially relevant bones, particularly the ulna, are incomplete, making comprehensive study of limb function impossible.

Recent molecular phylogenetic studies (Willows-Munro and Matthee, 2009; Taylor et al., 2013) indicate that the genus *Myosorex* is paraphyletic with respect to the genus *Congosorex* and suggest a higher level of taxonomic diversity within *Myosorex* than is currently recognized. While this arrangement implies that some of the morphological differences we document in *Myosorex* may relate to older divergences than indicated by current taxonomy, it also makes it more difficult to understand the unique skeletal proportions of *C. phillipsorum* as a consequence of phylogeny. The phylogenetic positions of *Congosorex* and *M. zinki* as successive outgroups to a South African clade of *Myosorex* (Taylor et al., 2013) suggest a complex history of locomotory evolution within a *Congosorex-Myosorex* clade.

ACKNOWLEDGMENTS

The authors thank R. Hutterer, who drew attention to the interesting skeletal morphology of *Surdisorex* and motivated us to begin our study of the myosoricine postcranial skeleton. The authors are grateful to W. T. Stanley and J. C. Kerbis Peterhans for graciously permitting us to examine recently-collected specimens of poorly documented species that resulted from their field work. The following curators and collections managers permitted us to study specimens under their care: N. B. Simmons, R. S. Voss, and E. Westwig (AMNH); L. R. Heaney, B. D. Patterson, and W. T. Stanley (FMNH). A. L. Gardner and two anonymous reviewers provided valuable comments on previous versions of this manuscript. Any use of trade, product, or firm names is for descriptive purposes only and does not imply endorsement by the United States government.

APPENDIX : SPECIMENS EXAMINED

Specimens examined for this study are deposited in the following institutions: American Museum of Natural History, New York (AMNH); Field Museum of Natural History, Chicago (FMNH); National Museum of Natural History, Washington United States National Museum of Natural History (USNM). Symbols: *, no skeleton available; †, manus and pes measurements could not be obtained.

Soricidae:

Congosorex phillipsorum ($n = 7$). Tanzania: Iringa District (FMNH 177683–177689).

Myosorex blarina ($n = 3$). Uganda: Kasese District (FMNH 144209, 144211). Zaire: Ruwenzori (FMNH 26285*).

Myosorex cafer ($n = 2$). South Africa: Kwazulu Natal Prov. (FMNH 165585, 165587).

Myosorex geata ($n = 12$). Tanzania: Kilosa District (FMNH 166767, 166775, 166777, 197667, 197670–197673); Morogoro District (FMNH 158299–158302); Mpwapwa District (FMNH 166767).

Myosorex kihaulei ($n = 12$). Tanzania: Kilombero District (FMNH 155620–155622); Makete District (FMNH 204685, 204856, 204858, 204860, 204862); Rungwe District (FMNH 163552, 163554, 163558, 163559).

Myosorex varius ($n = 5$). South Africa: Kwazulu Natal Prov. (FMNH 165588†, 165589–165592).

Myosorex zinki ($n = 2$). Tanzania: Kilimanjaro Region (FMNH 174117, 174119).

Surdisorex norae ($n = 21$). Kenya: Aberdare Mountains (AMNH 187262; FMNH 190622–190624, 190625†, 190626; USNM 182581*–182586*, 589811–589813, 589814†, 589815, 589816†, 589817, 589818†, 589819*).

Surdisorex polulus ($n = 23$). Kenya: Mount Kenya (USNM 163975*, 163976*, 163979*, 163981*, 163982*, 163984*, 163987*, 163989*–163991*, 163993*, 163996*–164000*, 164002*–164007*, 589820).

Talpidae:

Neurotrichus gibbsii gibbsii ($n = 26$). USA: Oregon (USNM 13410*, 65707*, 79788*, 80217*, 80437*–80441*, 89023*, 204484*–204487*, 264887*, 557433†–557435†,557437†, 557451†, 557460†–557463†, 560096†). Washington (USNM 273085†).

Uropsilus soricipes ($n = 10$). China: Sichuan (USNM 175142*, 256119, 260743*, 260751*, 574297, 574298*–574301*, 574302†).

LITERATURE CITED

Bell CJ, Mead JI. 2014. Not enough skeletons in the closet: Collections-based anatomical research in an age of conservation conscience. Anat Rec 297:344–348.

Churchfield S. 1990. The Natural History of Shrews. Ithaca, NY: Comstock Publishing Associates.

Coe MJ, Foster JB. 1972. The mammals of the northern slopes of Mt. Kenya. J East Afr Nat Hist Soc Natl Mus 131:1–18.

Duncan P, Wrangham RW. 1971. On the ecology and distribution of subterranean insectivores in Kenya. J Zool 164:149–163.

Edwards LF. 1937. Morphology of the forelimb of the mole (*Scalops aquaticus*, L.) in relation to its fossorial habits. Ohio J Sci 37:20–41.

Eisenberg JF. 1981. The Mammalian Radiations. Chicago, IL: The University of Chicago Press.

Elissamburu A, De Santis L. 2011. Forelimb proportions and fossorial adaptations in the scratch-digging rodent *Ctenomys* (Caviomorpha). J Mammal 92:683–689.

Hildebrand M. 1985a. Walking and running. In: Hildebrand M, Bramble DM, Liem KF, Wake DB, editors. Functional Vertebrate Morphology. Cambridge, MA: Belknap Press. pp 38–57.

Hildebrand M. 1985b. Digging of quadrupeds. In: Hildebrand M, Bramble DM, Liem KF, Wake DB, editors. Functional Vertebrate Morphology. Cambridge, MA: Belknap Press. pp 89–109.

Hopkins SSB, Davis EB. 2009. Quantitative morphological proxies for fossoriality in small mammals. J Mammal 90: 1449–1460.

Hutterer R. 1985. Anatomical adaptations of shrews. Mamm Rev 15:43–55.

Hutterer R. 2005. Order Soricomorpha. In: Wilson DE, Reeder DM, editors. Mammal Species of the World: A Taxonomic and Geographic Reference, 3rd ed. Baltimore, MD: The Johns Hopkins University Press. pp 220–311.

Kerbis Peterhans JC, Hutterer R, Kaliba P, Mazibuko L. 2008. First record of *Myosorex* (Mammalia: Soricidae) from Malawi with description as a new species, *Myosorex gnoskei*. J East Afr Nat Hist 97:19–32.

Kerbis Peterhans JC, Stanley WT, Hutterer R, Demos TC, Agwanda B. 2009. A new species of *Surdisorex* Thomas, 1906 (Mammalia, Soricidae) from western Kenya. Bonn Zool Beit 56:175–183.

Kerbis Peterhans JC, Hutterer R, Mwanga J, Ndara B, Davenport L, Karhagomba I, Udelhoven J. 2010. African shrews endemic to the Albertine Rift: Two new species of *Myosorex* (Mammalia: Soricidae) from Burundi and the Democratic Republic of Congo. J East Afr Nat Hist 99:103–128.

Kerbis Peterhans JC, Huhndorf MH, Plumptre AJ, Hutterer R, Kaleme P, Ndara B. 2013. Mammals, other than bats, from the Misotshi-Kabogo highlands (eastern Democratic Republic of Congo), with the description of two new species (Mammalia: Soricidae). Bonn Zool Bull 62:203–219.

Kirk EC, Lemelin P, Hamrick MW, Boyer DM, Bloch JI. 2008. Intrinsic hand proportions of euarchontans and other mammals: Implications for the locomotor behavior of plesiadapiforms. J Hum Evol 55:278–99.

Klietmann J, Nagel D, Rummel M, van den Hoek Ostende LW. 2014. *Heterosorex* and Soricidae (Eulipotyphla, Mammalia) of the fissure Petersbuch 28; micro-evolution as indicator of temporal mixing? C R Palevol 13:157–181.

Lemelin P. 1999. Morphological correlates of substrate use in didelphid marsupials: Implications for primate origins. J Zool 247:165–175.

Martin, T. 2005. Postcranial anatomy of *Haldanodon exspectatus* (Mammalia, Docodonta) from the Late Jurassic (Kimmeridgian) of Portugal and its bearing for mammalian evolution. Zool J Linn Soc 145:219–248.

Meester J. 1953. The genera of African shrews. Ann Transvaal Mus 22:205–214.

Meredith RW, Janečka JE, Gatesy J, Ryder OA, Fisher CA, Teeling EC, Goodbla A, Eizirik E, Simao TL, Stadler T, Rabosky DL, Honeycutt RL, Flynn JJ, Ingram CM, Steiner C, Williams TL, Robinson TJ, Burk-Herrick A, Westerman M, Ayoub NA, Springer MS, Murphy WJ. 2011. Impacts of the Cretaceous terrestrial revolution and KPg extinction on mammal diversification. Science 334:521–524.

Price MV. 1993. A functional–morphometric analysis of forelimbs in bipedal and quadrupedal heteromyid rodents. Biol J Linn Soc 50:339–360.

Quérouil S, Hutterer R, Barrière P, Colyn M, Kerbis Peterhans JC, Verheyen E. 2001. Phylogeny and evolution of African shrews (Mammalia: Soricidae) inferred from 16s rRNA sequences. Mol Phylogenet Evol 20:185–195.

Reed CA. 1951. Locomotion and appendicular anatomy in three soricoid insectivores. Am Midl Nat 45:513–670.

Samuels JX, Van Valkenburgh B. 2008. Skeletal indicators of locomotor adaptations in living and extinct rodents. J Morphol 269:1387–1411.

Sanchez-Villagra MR, Menke PR, Geisler JH. 2004. Patterns of evolutionary transformation in the humerus of moles (Talpidae, Mammalia): A character analysis. Mamm Study 29:163–170.

Sargis EJ. 2002. Functional morphology of the forelimb of tupaiids (Mammalia, Scandentia) and its phylogenetic implications. J Morphol 253:10–42.

Sargis EJ, Woodman N, Reese AT, Olson LE. 2013a. Using hand proportions to test taxonomic boundaries within the *Tupaia glis* species complex (Scandentia, Tupaiidae). J Mammal 94:183–201.

Sargis EJ, Woodman N, Morningstar NC, Reese AT, Olson LE. 2013b. Morphological distinctiveness of Javan *Tupaia hypochrysa* (Scandentia, Tupaiidae). J Mammal 94:938–947.

Shimer HW. 1903. Adaptations to aquatic, arboreal, fossorial and cursorial habits in mammals. III. Fossoriality. Am Nat 37:819–825.

Stanley WT, Rogers MA, Hutterer R. 2005. A new species of *Congosorex* from the Eastern Arc Mountains, Tanzania, with significant biogeographical implications. J Zool 265: 269–280.

Stein BA. 2000. Morphology of subterranean rodents. In: Lacey EA, Patton JL, Cameron GN, editors. Life Underground. The Biology of Subterranean Rodents. Chicago, IL: The University of Chicago Press. pp 19–61.

Taylor PJ, Kearney TC, Kerbis Peterhans JC, Baxter RM, Willows-Munro S. 2013. Cryptic diversity in forest shrews of the genus *Myosorex* from southern Africa, with the description of a new species and comments on *Myosorex tenuis*. Zool J Linn Soc 169:881–902.

Vizcaino SF, Milne N. 2002. Structure and function in armadillo limbs (Mammalia: Xenarthra: Dasypodidae). J Zool 257:117–127.

Weisbecker V, Schmid S. 2007. Autopodial skeletal diversity in hystricognath rodents: Functional and phylogenetic aspects. Mamm Biol 72:27–44.

Weisbecker V, Warton DI. 2006. Evidence at hand: Diversity, functional implications, and locomotor prediction in intrinsic hand proportions of diprotodontian marsupials. J Morphol 267:1469–1485.

Willows-Munro S, Matthee CA. 2009. The evolution of the southern African members of the shrew genus *Myosorex*: Understanding the origin and diversity of a morphologically cryptic group. Mol Phylogenet Evol 51:394–398.

Willows-Munro S, Matthee CA. 2011. Exploring the diversity and molecular evolution of shrews (family Soricidae) using mtDNA cytochrome *b* data. Afr Zool 46:246–262.

Woodman N, Gaffney SA. 2014. Can they dig it? Functional morphology and degrees of semifossoriality among some American shrews (Mammalia, Soricidae). J Morphol 275:745–759.

Woodman N, Morgan JJP. 2005. Skeletal morphology of the fore foot in shrews (Mammalia: Soricidae) of the genus *Cryptotis*, as revealed by digital x-rays. J Morphol 266:60–73.

Woodman N, Stabile FA. 2015. Variation in the myosoricine hand skeleton and its implications for locomotory behavior (Eulipotyphla: Soricidae). J Mamm 96.

Woodman N, Stephens RB. 2010. At the foot of the shrew: Manus morphology distinguishes closely-related *Cryptotis goodwini* and *Cryptotis griseoventris* (Mammalia, Soricidae) in Central America. Biol J Linn Soc 99:118–134.